EPJ Appl. Metamat. **8**, 5 (2021)

https://doi.org/10.1051/epjam/2020017

EPJ Applied Metamaterials

Available online at:
epjam.edp-open.org

RESEARCH ARTICLE OPEN ACCESS

A miniaturized frequency selective rasorber with high selectivity passband and wideband absorption properties

Yanjie Wu[1], Jie Xiong[1,2,*], Feng Deng[3], Hai Lin[1,**], and You Wang[1]

[1] College of Physics Science and Technology, Central China Normal University, Wuhan 430079, PR China
[2] School of Physics and Telecommunications, HuangGang Normal University, Huanggang 438000, PR China
[3] Science and Technology on Electromagnetic Compatibility Laboratory, China Ship Development and Design Centre, Wuhan 430000, PR China

Received: 30 November 2020 / Accepted: 24 December 2020

Abstract. A miniaturized frequency selective rasorber (FSR) with high selectivity passband and wideband absorption properties is presented. Its performance as an absorber over a wide absorption band from 8.08 to 18.08 GHz through the structure of metal incurved square loop structure loaded resistors. The frequency selective surface (FSS) using Jerusalem cross array and metallic patch realizes the transmission frequency band from 2.7 to 3.52 GHz. And the insertion loss (IL) is 0.37 dB at 3.08 GHz. The symmetry and miniaturized elements design enable the proposed FSR to achieve satisfactory incident angle stability. Its small unit size effectively avoids the generation of grating lobes in the absorption band and the interference to Radar Cross Section (RCS) reduction.

Keywords: Frequency selective rasorber / frequency selective surface / miniaturized elements / grating lobes / radar cross section

1 Introduction

In recent years, with the rapid development of metamaterials and metasurfaces, many technologies have been reported to improve the electromagnetic performance of radomes [1–8]. Frequency selective surface (FSS) is a two-dimensional planar periodic structure composed of a specific arrangement of resonance units. It can effectively control the reflection and transmission characteristics of electromagnetic waves, and is often used as a spatial filter [9,10]. The traditional radome uses band-pass FSS to ensure the transmission of the antenna within the operating band and reflect out-of-band energy, but it cannot absorb electromagnetic wave energy. In order to solve this imperfection, frequency selective rasorber (FSR) with transmission/absorption characteristics has been proposed and attracted widespread attention [11]. Unlike traditional FSS radomes, FSR will transmit incident electromagnetic singles within the passband and absorb out-of-band signals, which can effectively reduce Radar Cross Section (RCS) [12,13]. Therefore, FSR is very useful for stealth radome system and mutual interference reduction system [14].

In recent years, in order to better explore the wave absorption and transmission characteristics of FSR, researchers have carried out extensive research on FSR and taken different ways to design the FSR. For example, in [15], a FSR with metal square ring array and interdigitated Jerusalem cross elements was proposed. The FSR structure realizes the electromagnetic characteristics of low-frequency transmission and high-frequency absorption. Later, to enhance the flexibility and application scope of FSR, some more complicated structures were designed. Such as FSRs with two-sided absorption bands reported in [16–19], FSRs with high-frequency passband reported in [20–23], and employing the 3D FSS concept proposed in [24–27]. However, 3D FSR structures are usually more complex and require a higher cost to fabricate. So it is difficult to conform with the configuration of the antenna system.

Different types of FSRs should meet individual requirements under different application scenarios. Currently, the main development region of FSR is still lower insertion loss (IL) and wider absorption bandwidth. To widen the absorption bandwidth, it is often proposed by using lumped resistor loaded FSS [28–30]. In [28], square

* e-mail: xiongjie82@mails.ccnu.edu.cn
** e-mail: linhai@mail.ccnu.edu.cn

loops loaded with lumped resistors were used to expand the absorbing bandwidth, and meandering square slots with a smaller period were used to realize the transmission characteristics. In order to achieve better transmitting characteristics in the low frequency band, the method of loading lumped capacitors on the Jerusalem cross was proposed in [29]. However, this method is easy to produce grating lobes in the high frequency part. In [30], a square structure loaded with eight resistors was proposed to realize the absorbing characteristics mainly in the C-band. In [31], the metallic FSS was used as the ground plane of a thin wideband absorber based on resistive high-impedance surfaces within the total reflection band. Its −10 dB absorption bandwidth ranges are 10–18 GHz. In [32], a multilayer design is used to obtain smaller cell size, thus avoiding the problems of gate lobe and parasitic passband. Unfortunately, none of the above 2D structures can achieve ultra-wideband absorption in X, Ku band while achieving low IL in low-frequency transmission bands. Several miniaturized 3D FSR structures with broad absorption bandwidth were proposed in [33,34]. However, due to its 3D structure, which is normally difficult to fabricate and don't precise assembly. And their IL was higher than 0.5 dB.

Compared with previous research works, in this paper, we proposed a miniaturized FSR design which has ultrawide absorption band along with low IL bandpass. Finally, we realize the lower IL of 0.37 dB at 3.08 GHz and −10 dB absorption ranges from 8.04 to 18.08 GHz. Namely, its fractional bandwidth (FBW) is 77%. It is worth mentioning that the unit size of the designed FSR is finally miniaturized to only 7 mm. As a result, its small unit size avoids the generation of grating lobes in the absorbing band and thus avoids its interference with RCS reduction. On the other hand, it has good angular stability under oblique incident.

2 Design and analysis of the FSR

Figure 1a illustrates the three-dimensional configuration of the designed 2D-FSR. It consists of a lossy FSS layer and a lossless FSS layer which is separated by a 3.5-mm-thick air spacer. For the lossy layer, the metal incurved square loop that loads four lumped resistors with a 115 Ω resistance to form a wideband absorption FSS. Its unit size is only 4.9 mm × 4.9 mm. For the lossless layer, it is synthesized by Jerusalem cross array on the upper surface of the lossless FSS layer substrate and capacitive metal patch on the lower surface of the substrate. Both of them construct high selective band-pass FSS in low frequency band. Both the lossy layer and the lossless layer are printed on the Rogers R04350B substrate. Its thickness, loss tangent, and relative permittivity are 0.508 mm, 0.0037, and 3.48, respectively. The structure parameters of the unit cell are given in Table 1.

It should be noted that the unit size of the proposed FSR is very small. The smaller size can suppress the high-frequency grating lobes and avoid interference to the absorption bandwidth. However, with the reduction of cell size, the transmission window will move to the high frequency region. Since the designed transmission band is in S-band, the traditional FSS period size is generally larger, while the absorption band is in X and Ku bands, so the period of lossless layer is larger than that of lossy layer. It is well known that larger period size often leads to grating lobes in the high frequency part of the absorption band, and the stability of grating lobes decreases with the increase of incident angle. However, in the high frequency part, the lumped capacitance is easy to be broken down, and there will be more interference. In order to solve the above problems, we use the method of adding a capacitive metal patch in the bottom layer to replace lumped capacitance.

Equivalent impedance theory is an important physical method to study the absorbing characteristics. It can be

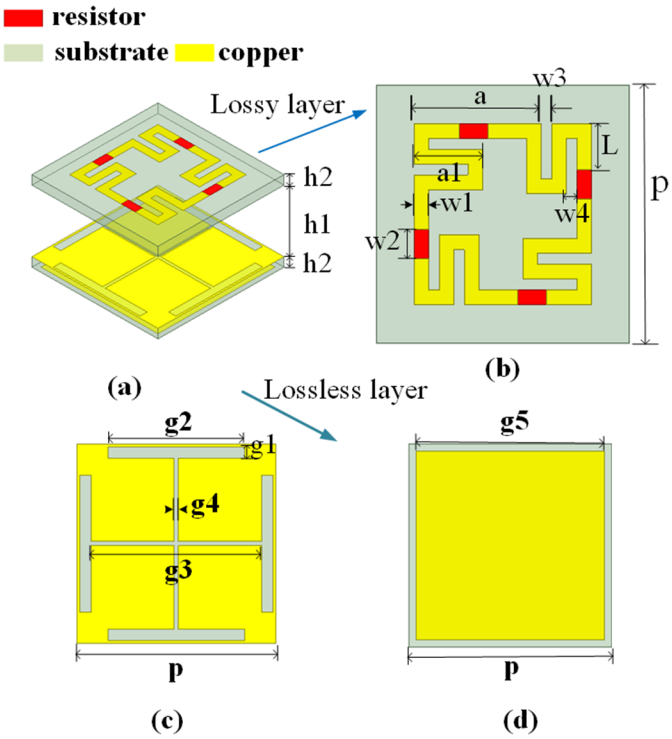

Fig. 1. Topology and dimensions of proposed FSR. (a) Three-dimensional structure diagram of proposed FSR. (b) Lossy layer. (c) Upper surface structure of lossless layer: Jerusalem cross. (d) Lower surface structure of lossless layer: Capacitive metal patch.

Table 1. Parameters of the proposed FSR.

Parameter	Value (mm)	Parameter	Value (mm)
p	7	g1	0.4
a	3.5	g2	4.8
w1	0.4	g3	6
w2	0.8	g4	0.15
w3	0.3	g5	6.5
w4	0.3	h1	3.5
a1	1.9	h2	0.508
L	1.25		

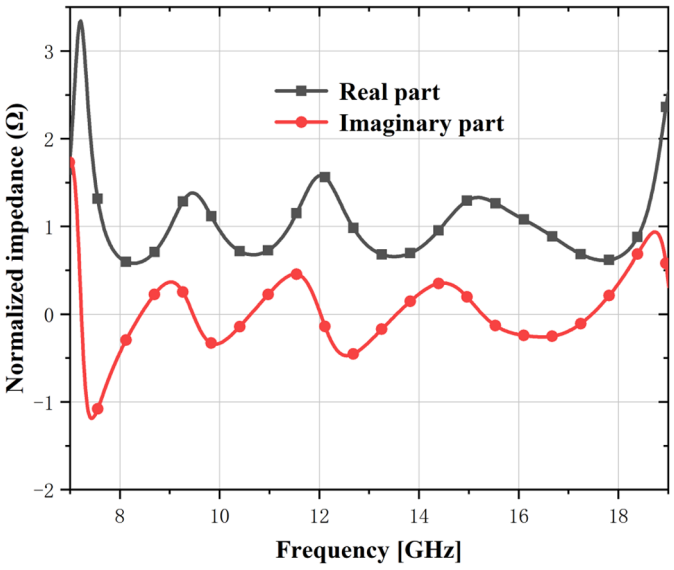

Fig. 2. Normalized impedance of the proposed FSR.

calculated by S parameter:

$$Z = \sqrt{\frac{(1+S_{11})^2 - S_{21}^2}{(1-S_{11})^2 - S_{21}^2}}$$

where Z is the equivalent impedance of FSR, S_{11} is the reflection coefficient, and S_{21} is the transmission coefficient. When FSR works in the absorption band, it is used as an absorber. When the incident wave is completely absorbed, the reflection coefficient and transmission coefficient are both 0. At this time, $Z = 1$, which means perfect wave absorption.

As shown in Figure 2, we have studied the normalized impedance Z of the absorbing part of the proposed FSR. It can be clearly observed from the figure that in the 8.04–18.08 GHz band, the real part of the equivalent impedance Z fluctuates slightly near 1, and the imaginary part fluctuates slightly near 0. This means that the real and imaginary parts of the equivalent impedance of the FSR have good impedance matching with the free space. Hence the FSR has good absorbing characteristics in this frequency band.

Furthermore, we have studied the surface current distribution with R and without R in three resonant frequencies (3, 9.5 and 16.5 GHz) and analyzed the working principle of the FSR. As shown in Figure 3, the color map shows that at 3 GHz, with or without resistance R, a strong current distribution appears in the lossless layer, while the current is very weak in the lossy layer. This indicates that the lossless layer forms a parallel resonance at 3 GHz and generates an infinite impedance. But there is no response to incident electromagnetic waves in the lossy layer. Therefore, the designed FSR has better transmission performance and lower IL. However, since the electromagnetic wave has to pass through the two-layer dielectric substrate, the IL is inevitable and can only be reduced, but cannot be completely eliminated.

When the incident electromagnetic waves are at 9.5 and 16.5 GHz, their surface current distribution is exactly

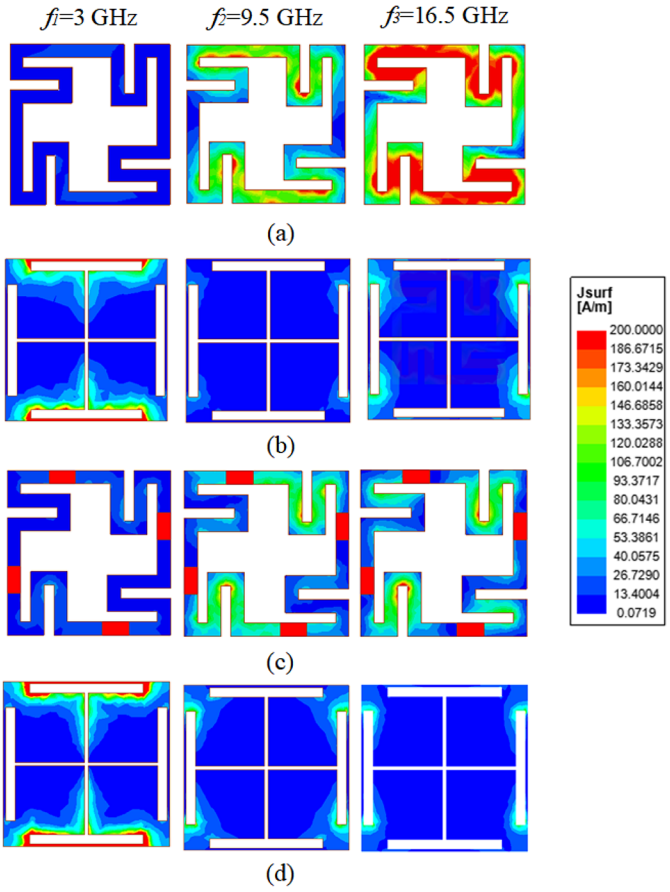

Fig. 3. The surface current distribution of the lossy layer and lossless layer with R and without R at $f_1 = 3$ GHz, $f_2 = 9.5$ GHz, $f_3 = 16.5$ GHz, respectively. (a) Current distribution of lossy layer without R. (b) Current distribution of lossless layer without R. (c) Current distribution of lossy layer with R. (d) Current distribution of lossless layer with R.

opposite to that at 3 GHz. When there is no lumped resistance, the lossy layer current distribution is stronger on the long side perpendicular to the electric field direction, which shows that 9.5 and 16.5 GHz are two series resonance points on the FSR. In order to achieve a better absorbing effect, we place the lumped resistor at the position with strong current distribution. After the lumped resistance is loaded, the current on the sides of the square ring is effectively absorbed by bending.

3 Performance of the FSR

In order to analyze the performance of the designed FSR, we used numerical simulation software to simulate the designed FSR. When electromagnetic waves are perpendicularly incident, the simulated reflection/transmission coefficient and absorptivity of the designed FSR are shown in Figure 4. The absorption parameter $A(f)$ can be calculated from the S parameter as [35,36] $A(f) = 1 - T(f) - R(f) = 1 - |S_{21}|^2 - |S_{11}|^2$. In order to achieve better absorption performance, a smaller reflection/transmission coefficient is required. Therefore, by optimizing the

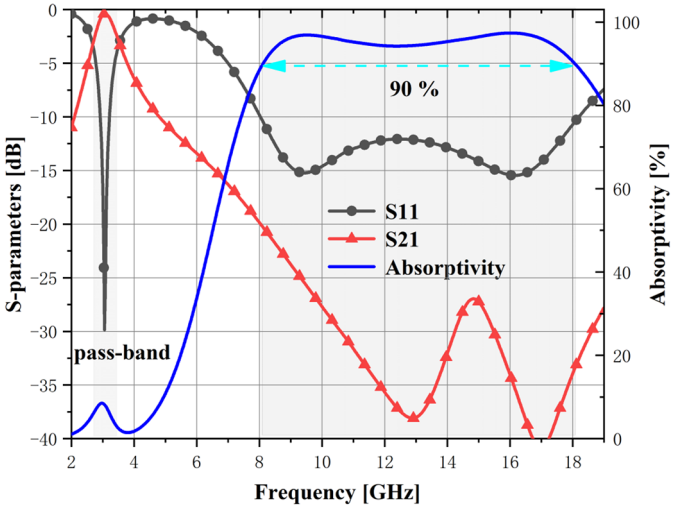

Fig. 4. S-parameter results and absorptivity of the designed FSR.

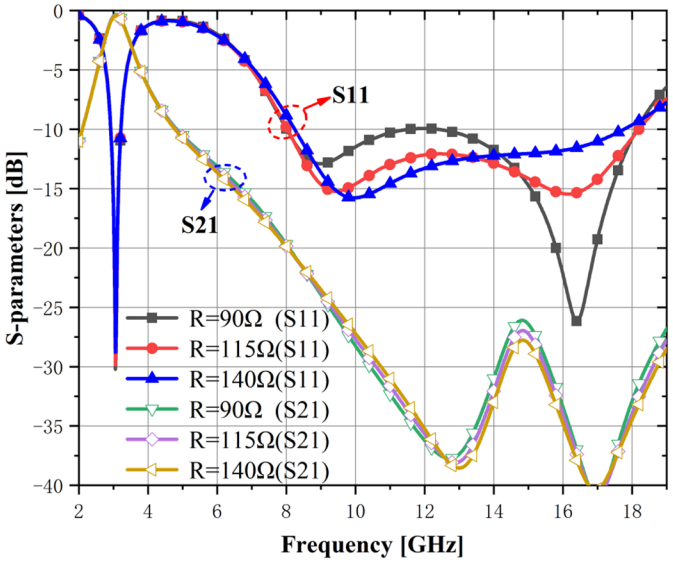

Fig. 5. S-parameter results of the designed FSR with different R.

parameters, we can see from Figure 4, that the passband range of the −3 dB bandwidth of the structure is 2.7–3.52 GHz. At 3.08 GHz, the IL is only 0.37 dB, and the transmission bandwidth is about 800 MHz. Achieved an −10 dB absorption band of 8.04–18.08 GHz with a relative absorber bandwidth of 77.23%. And between 8.04 and 18.08 GHz, the absorptivity is higher than 90%.

In general, the key parameter that affects the absorption performance of FSR is the resistance R of the lumped resistor. In order to make the designed FSR obtain the best absorption performance under the condition of small IL, we optimized the value of different resistance R. Figure 5 illustrates the simulation results of the design FSR with different resistance values. It can be observed that the influence of resistance on the reflection coefficient is greater than the influence on the transmission coefficient. When the resistance value is 90 Ω and 140 Ω, the absorption effect is significantly worse than that of 115 Ω. It also shows that the impedance matching is better at 115 Ω.

Figure 6 illustrates the simulated reflection/transmission coefficients of the designed FSR for different incident angles under dual polarization conditions. It can be seen that as the incident angle increases, from 0° to 45°, the absorption characteristics of the designed FSR have little change, and still maintains high absorption performance under different oblique incident angles.

Figure 7 shows the simulated reflection/transmission coefficients for different incident angles under TE polarization and TM polarization. With the increase of the incident angle, the transmission performance of the low frequency band changes little. For the absorption band of 8.04–18.08 GHz, within 45°, the absorption performance under TE polarization hardly changes. When the oblique incident angle is 45°, the absorption band shifts upward as a whole. However, under TM polarization, the absorption band bandwidth begins to narrow at 30°, and at 45° oblique incidence, a grating lobe appears in S21. The reason for this situation is that under TM polarization, when the incident angle is large, the impedance mismatch causes the decrease

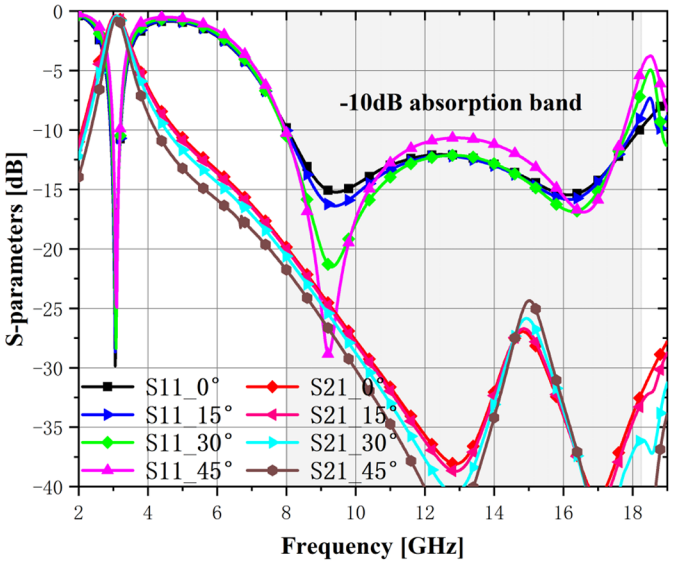

Fig. 6. S-parameter of the designed FSR for different incident angles under dual polarization conditions.

of the absorption performance. However, under the simultaneous action of the two polarizations, a high absorptivity can still be maintained. Hence, it can be observed that the designed FSR has good incident angle stability.

4 Experimental verification

In order to verify the performance of the designed FSR, a prototype of the presented FSR was fabricated and measured. As shown in Figure 8a, the prototype contains 80 × 60 units with a size of 560 mm × 420 mm × 4.516 mm.

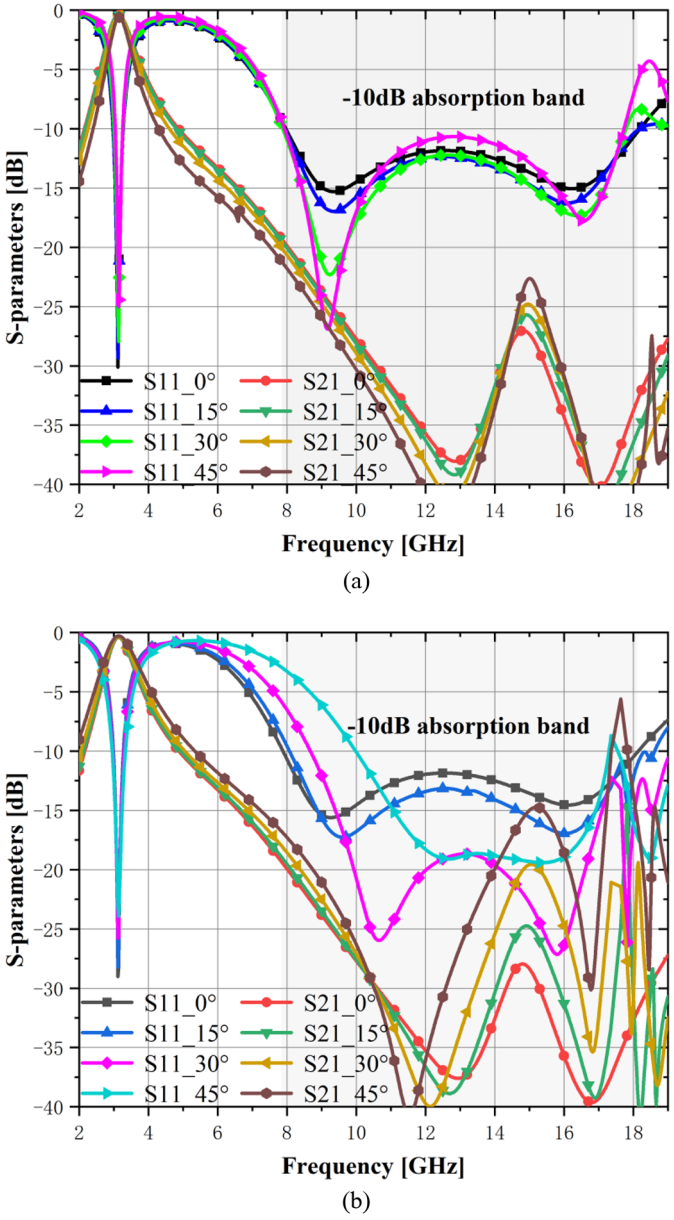

Fig. 7. S-parameter of the designed FSR for different incident angles under (a) TE polarization, (b) TM polarization.

There are four lumped resistors are welded on each lossy unit cell, these resistors have a 115 Ω resistance and a 0603 package. Similarly, in the middle of the two layers of the substrate is separated by the polymethacrylimide (PMI) foam with $\varepsilon_r = 1.1$ to ensure a distance of 3.5 mm.

The fabricated FSR prototype was embedded in the center of the fixture on the surface of the absorption material. As shown in Figure 8b, the fixture is between the transmitting antennas and the receiving antenna connected to the vector network analyzer (Agilent E8362B). It is used to simulate the incidence of electromagnetic waves to test the S-parameter of the prototype. The test frequency range is from 1 to 20 GHz. And measurement and simulation comparison of S-parameters and absorptivity of FSR prototype under normal incidence is shown in Figure 9. It can be clearly observed that the measured

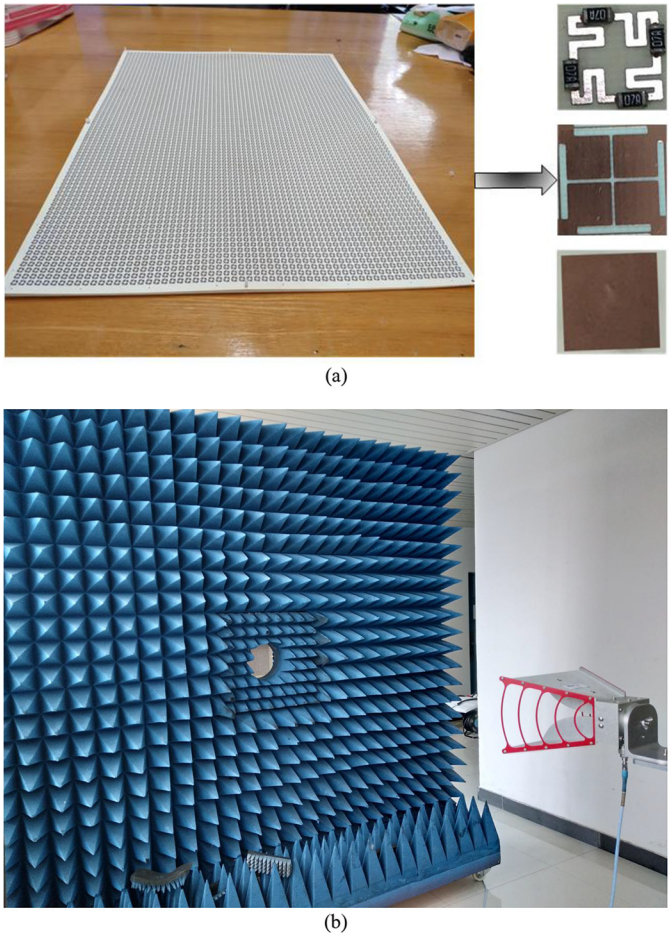

Fig. 8. (a) Prototype of the manufactured FSR. (b) Photograph of the measuring setup.

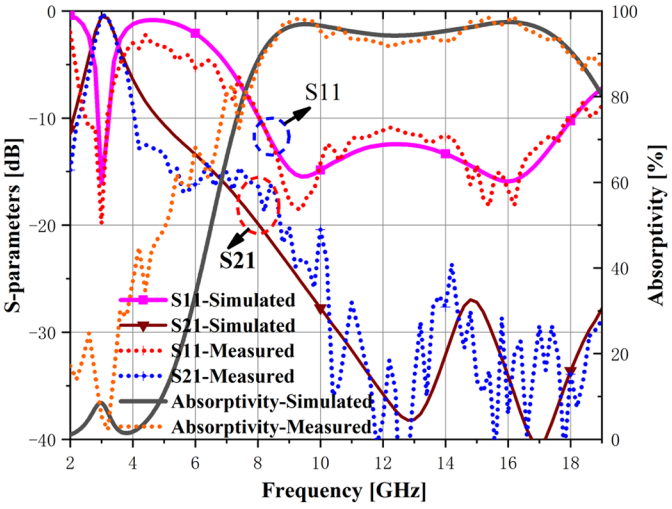

Fig. 9. Measurement and simulation comparison of S-parameters and absorptivity of FSR prototype under normal incidence.

results and simulated results have a good agreement. The IL of the transmission band is 0.37 dB at 3.08 GHz, and the measured −10 dB absorption bandwidth range is from

Table 2. Performance comparisons between the designed FSR and some FSRs in references.

References	Transmission band (GHz)/IL (dB)	−10 dB absorption band (GHz)/FBW	Thickness (λ_p^1)	Periodicity (mm)	Form
[28]	6/−0.8	10.6–18/52%	0.074	11 × 11	2D
[29]	1.6/NA[2]	5.3–14.8/94%	0.024	10 × 10	2D
[30]	0.92/−0.5	3–9/100%	0.03	20 × 20	2D
[31]	4.6/−0.3	10–18/57%	0.08	11 × 11	2D
[32]	2.45/−1.2	7.68–21.7/95.2%	0.107	5 × 5	2D
[33]	4.15/−2.4	4.8–9.3/64%	0.065	NA	3D
[34]	3.4/−1.2	11.1–18/47.4%	0.054	8 × 8	3D
This work	3.08/−0.37	8.04–18.08/77%	0.036	7 × 7	2D

[1]λ_p is free space wavelength at the center frequency of transmission band.
[2]NA means the data in the paper are not given.

8.0 to 18.1 GHz. And between 8.0 and 18.1 GHz, the absorptivity is higher than 90%. The difference between the simulation and the measurement may be due to inaccuracies in the spacing between the two layers, the instability in the relative permittivity of the substrate and other manufacturing errors.

Finally, in order to better illustrate the advantages of the proposed FSR in this article, we compared the designed FSR with other published in Table 2. It is observed from the table that the FSR we designed has a lower IL in the low frequency range and a high absorption bandwidth in the high frequency range, which is difficult for works in other literatures. Moreover, the periodicity of the designed FSR in this paper is smaller, and it has fewer lumped resistors.

5 Conclusion

In this paper, a miniaturized FSR with high selectivity passband and wideband absorption properties is designed. A Jerusalem cross aperture array and capacitive metal patch are used to generate of the high selective passband and reduce the unit size. Its miniaturization of FSS avoids grating lobes impact on high-frequency absorption performance. To implement the ultrawide absorption, a metal incurved square loop structure loaded with lumped resistances was chosen as the absorbing unit. This proposed FSR has a lower IL of 0.37 dB at 3.08 GHz and a wide absorption band ranges from 8.04 to 18.08 GHz (77%). The period unit size of proposed FSR is only 7 mm × 7 mm × 3.5 mm, that is, 0.072 λ_p × 0.072 λ_p × 0.036 λ_p (λ_p is free space wavelength at the center frequency of transmission band). And the FSR achieves stable absorbing performance under oblique incident, which is desirable for practical applications of the stealth radome. Finally, a prototype of the proposed FSR was manufactured and measured, and the measurement results are in agreement with the simulation results.

This research was funded by the fundamental Research Funds for the Central University of China under grant "CCNU18JCXK02, CCNU18GF006, CCNU16A02016, CCNU19TS073"; the open fund of Guangxi Key Laboratory of wireless wideband communication and Signal Processing under grant "GXKL06190202"; the open fund of China Ship Development and Design Centre under grant "XM0120190196"; funded in part by the Beijing Orient Institute of Measurement and Test Electrostatic Research Foundation of Liu Shanghe Academicians and Experts Workstation under Grant BOIMTLSHJD20181002.

References

1. T.J. Cui, L. Li, S. Liu, Q. Ma, L. Zhang, X. Wan et al., Information metamaterial systems, iScience **23**, 101403 (2020)
2. L. Zhou, Z. Shen, Absorptive coding metasurface with ultrawideband backscattering reduction, IEEE Antennas Wirel. Propag. Lett. **191**, 201 (2020)
3. R. Phon, S. Lim, Dynamically self-reconfigurable multifunctional all-passive metasurface, ACS Appl. Mater. Interfaces **12**, 42393 (2020)
4. P. Fei, G.A.E. Vandenbosch, W. Guo, X. Wen, D. Xiong, W. Hu et al., Versatile cross-polarization conversion chiral metasurface for linear and circular polarizations, Adv. Opt. Mater. **8**, 10 (2020)
5. B.A. Munk, *Frequency selective surfaces: theory and design* (John Wiley & Sons, 2005)
6. N.I. Landy, S. Sajuyigbe, J.J. Mock, D.R. Smith, W.J. Padilla, Perfect metamaterial absorber, Phys. Rev. Lett. **100**, 207402 (2008)
7. B.A. Munk, *Metamaterials: critique and alternatives* (John Wiley & Sons, 2009)
8. V.S. Asadchy, A. Díaz-Rubio, S.A. Tretyakov, Bianisotropic metasurfaces: physics and applications, Nanophotonics **7**, 1069 (2018)
9. R. Mittra, C.H. Chan, T. Cwik, Techniques for analyzing frequency selective surfaces-a review, Proc. IEEE **76**, 1593 (1988)
10. X. Sheng, J. Fan, N. Liu, C. Zhang, A dual-band fractal FSS with SZ curve elements, IEICE Electron. Express **14**, 20170518 (2017)
11. W.S. Arceneaux, R.D. Akins, W.B. May, Absorptive/transmissive radome, US Patent 5,400,043, 1995
12. W. Jiang, Y. Liu, S. Gong, T. Hong, Application of bionics in antenna radar cross section reduction, IEEE Antennas Wirel. Propag. Lett. **8**, 1275 (2009)

13. Y. Liu, K. Li, Y. Jia, Y. Hao, S. Gong, Y.J. Guo, Wideband RCS reduction of a slot array antenna using polarization conversion metasurfaces, IEEE Trans. Antennas Propag. **64**, 326 (2015)
14. Y. Zhang, B. Li, L. Zhu, Y. Tang, Y. Chang, Y. Bo, Frequency selective rasorber with low insertion loss and dual-band absorptions using planar slotline structures, IEEE Antennas Wirel. Propag. Lett. **17**, 633 (2018)
15. L. Li-Guo, L. You-Quan, M. Qing-Zhi, W. Wei-Wei, M. Jin-Jun, F. Yun-Qi, Y. Nai-Chang, Design of an invisible radome by frequency selective surfaces loaded with lumped resistors, Chin. Phys. Lett. **30**, 064101 (2013)
16. K. Zhang, W. Jiang, S. Gong, Design bandpass frequency selective surface absorber using LC resonators, IEEE Antennas Wirel. Propag. Lett. **16**, 2586 (2017)
17. X. Xiu, W. Che, Y. Han, W. Yang, Low-profifile dual-polarization frequency-selective rasorbers based on simple-structure lossy cross-frame elements, IEEE Antennas Wirel. Propag. Lett. **17**, 1002 (2018)
18. X. Zhang, W. Wu, L. Huang, Y. Ma, N. Yuan, Design of dual-absorptive-bands frequency selective rasorber with minkowski loop arrays, IEEE Antennas Wirel. Propag. Lett. **18**, 1843 (2019)
19. Q. Guo, J. Su, Z. Li, L.Y. Yang, J. Song, Absorptive/transmissive frequency selective surface with wide absorption band, IEEE Access **7**, 92314 (2019)
20. Q. Chen, L. Liu, L. Chen, J. Bai, Y. Fu, Absorptive frequency selective surface using parallel LC resonance, Electron. Lett. **52**, 418 (2016)
21. Q. Chen, S. Yang, J. Bai, Y. Fu, Design of absorptive/transmissive frequency-selective surface based on parallel resonance, IEEE Trans. Antennas Propag. **65**, 4897 (2017)
22. Q. Chen, M. Guo, Z. Sun, D. Sang, Y. Fu, Polarization-independent frequency-selective rasorber with a broadened absorption band, Int. J. Electron. Commun. **96**, 178 (2018)
23. X. Chen, Y. Li, Y. Fu, N. Yuan, Design and analysis of lumped resistor loaded metamaterial absorber with transmission band, Opt. Express **20**, 28347 (2012)
24. D. Singh, R.P. Yadav, A 3-d printed square loop frequency selective surface for harmonic radar applications, J. Electromagn. Waves Appl. **34**, 396 (2020)
25. H. Huang, Z. Shen, A.A. Omar, 3-D absorptive frequency selective reflector for antenna radar cross section reduction, IEEE Trans. Antennas Propag. **65**, 5908 (2017)
26. Y. Yu, Z. Shen, T. Deng, G. Luo, 3-D frequency selective rasorber with wide upper absorption band, IEEE Trans. Antennas Propag. **65**, 4363 (2017)
27. T. Deng, Y. Yu, Z. Shen, Z.N. Chen, Design of 3-D multilayer ferrite-loaded frequency-selective rasorbers with wide absorption bands, IEEE Trans. Microw. Theory Tech. **67,** 108 (2018)
28. H. Li, Q. Cao, C. Yang, Y. Wang, Design and analysis of a frequency selective radome (FSR) with wideband absorbing properties, in *2016 IEEE International Workshop on Electromagnetics: Applications and Student Innovation Competition (iWEM)*, (IEEE, 2016), pp. 1–3
29. B. Yi, P. Liu, G. Li, Y. Dong, Design of miniaturized and ultrathin absorptive/transmissive radome with wideband absorbing property, Microw. Opt. Technol. Lett. **58**, 1870 (2016)
30. Q. Chen, J. Bai, L. Chen, Y. Fu, A miniaturized absorptive frequency selective surface, IEEE Antennas Wirel. Propag. Lett. **14**, 80 (2014)
31. F. Costa, A. Monorchio, A frequency selective radome with wideband absorbing properties, IEEE Trans. Antennas Propag. **60**, 2740 (2012)
32. L. Liu, H. Zhai, D. Hu, S. Ren, A polarization-stable frequency selective rasorber with miniaturized elements and wideband absorbing properties, Microw. Opt. Technol. Lett. **62**, 1643 (2020)
33. B. Li, Z. Shen, Wideband 3D frequency selective rasorber, IEEE Trans. Antennas Propag. **62**, 6536 (2014)
34. D. Hu, H. Zhai, L. Liu, J. Shi, Z. Nie, A new miniaturized frequency selective surface designed for Ku-band absorption and low-frequency bandpass, Microw. Opt. Technol. Lett. **62**, 315 (2020)
35. S.J. Li, P.X. Wu, H.X. Xu, Y.L. Zhou, X.Y. Cao, J.F. Han et al., Ultra-wideband and polarization-insensitive perfect absorber using multilayer metamaterials, lumped resistors, and strong coupling effects, Nanoscale Res. Lett. **13**, 386 (2018)
36. S.J. Li, Y.B. Li, H. Li, Z.X. Wang, C. Zhang, Z.X. Guo et al., A thin self-feeding Janus metasurface for manipulating incident waves and emitting radiation waves simultaneously, Ann. Phys. **532**, 13 (2020)

Cite this article as: Yanjie Wu, Jie Xiong, Feng Deng, Hai Lin, You Wang, A miniaturized frequency selective rasorber with high selectivity passband and wideband absorption properties, EPJ Appl. Metamat. **8**, 5 (2021)